

the black viscous oil which oozes from the Precambrian Nonesuch shale (15) using the procedures described and found that the members of the *n*-alkane series range from C₁₁ to about C₃₅. The distribution reaches a maximum around C₁₉ and there is a very slight, but quite definite, predominance of odd-numbered members. The branched-cyclic fraction (2.5 g), which still contains small amounts of aromatic hydrocarbon, is very complex, but is characterized by several prominent peaks in the region corresponding in retention time to that between *n*-C₁₄ and *n*-C₁₈ on the silicone gum column. We collected amounts of the order of a milligram for each of these peaks by successive sampling on a 6-mm column and then by rechromatographing these at 90°C upon a strongly polar substrate—5 percent tetracyanoethylated pentaerythritol on Gas-Chrom RA, 80–100 mesh, the column being 170 cm × 6 mm—that provided a particularly effective separation. Two of the fractions so obtained when chromatographed on a variety of substrates (Apiezon 'L', fluorosilicone QF-1, silicone gum SE-30, Carbowax-20M, and tetracyanoethylated pentaerythritol) gave single peaks of the same retention times as phytane and pristane. These identifications were then confirmed by direct comparison on the mass spectrometer (20).

The mass spectrometric data on incompletely separated fractions show that other compounds with isoprenoid skeletons are present; these fractions may represent geologic breakdown products from the more abundant phytane and pristane. Studies on a capillary column (with Apiezon 'L', 45 m × 0.25 mm at 170°C) of cuts taken from the packed columns show that the branched fraction is an extremely complex mixture: even so, the phytane and pristane comprise approximately 0.6 and 1.2 percent, respectively, of the branched-cyclic fraction.

If one accepts the presence of these hydrocarbons as evidence of life in Precambrian times, there remains the question of the relation between the oil and the rock. We believe that the oil is indigenous to the rock, since we have found an almost identical pattern for the normal and the branched-cyclic alkane fractions (about 3 mg total) isolated from carefully washed (water, HF, and benzene-methanol) and pulverized Nonesuch shale (18 g) taken from the so-called "marker bed" situated above the stratum from which the

oil had been collected. No method for the dating of ancient organic matter exists as yet, so that some doubt must remain concerning the precise age of this oil; however, the geologic evidence (15) favors the viewpoint that the organic matter and the associated copper are sedimentary or early diagenetic in origin.

GEOFFREY EGLINTON, P. M. SCOTT*

TED BELSKY, A. L. BURLINGAME

MELVIN CALVIN

Department of Chemistry, Lawrence Radiation Laboratory, and Space Sciences Laboratory, University of California, Berkeley

References and Notes

1. N. H. Horowitz and S. L. Miller, *Fortschr. Chem. Org. Naturstoffe* **20**, 423 (1962).
2. P. H. Abelson, *ibid.* **17**, 379 (1959); P. E. Cloud, Jr., and P. H. Abelson, *Proc. Natl. Acad. Sci. U.S.A.* **47**, 1705 (1961).
3. I. A. Breger, Ed., *Organic Geochemistry* (Macmillan, New York, 1963).
4. U. Colombo and G. D. Hobson, Eds., *Advances in Organic Geochemistry* (Macmillan, New York, 1964).
5. E. S. Barghoorn and S. A. Tyler, *Ann. N.Y. Acad. Sci.* **108**, 451 (1963); J. S. Harrington and P. D. Toens, *Nature* **200**, 947 (1963); C. G. A. Marshall, J. W. May, C. J. Perret, *Science* **144**, 290 (1964); A. G. Volodgin, *The Oldest Algae in the USSR* (Academy of Sciences of the U.S.S.R., Moscow, 1962).
6. W. G. Meinschein, *Space Sci. Rev.* **2**, 653 (1963).
7. P. H. Abelson, T. C. Hoering, P. L. Parker, in U. Colombo and G. D. Hobson (*4*, p. 169); J. E. Cooper and E. E. Bray, *Geochim. Cosmochim. Acta* **27**, 1113 (1963).
8. H. N. Dunning, in I. A. Breger (*3*), p. 367.
9. J. G. Bendoraitis, B. L. Brown, L. S. Hepner, *Anal. Chem.* **34**, 49 (1962); for other papers, J. J. Cummins and W. E. Robinson, *J. Chem. Eng. Data* **9**, 304 (1964).
10. M. Blumer, M. M. Mullin, D. W. Thomas, *Science* **140**, 974 (1963).
11. B. Hallgren and S. Larsson, *Acta Chem. Scand.* **17**, 543 (1963); G. Lamberts and R. T. Holman, *ibid.*, p. 281, and references cited therein.
12. J. D. Mold, R. K. Stevens, R. E. Means, J. M. Ruth, *Nature* **199**, 283 (1963).
13. W. Bergmann, in Breger (*3*), p. 534.
14. E. G. Curphey, *Petroleum, London* **15**, 297 (1952).
15. W. S. White and J. C. Wright, *Econ. Geol.* **49**, 675 (1954); W. S. White, *ibid.* **55**, 402 (1960).
16. J. G. O'Connor, F. H. Burow, M. S. Norris, *Anal. Chem.* **34**, 82 (1962).
17. J. D. Mold, R. K. Stevens, R. E. Means, J. M. Ruth, *Biochemistry* **2**, 605 (1963).
18. J. J. Cummins and W. E. Robinson, *J. Chem. Eng. Data* **9**, 304 (1964).
19. G. Eglinton and R. J. Hamilton, in *Chemical Plant Taxonomy*, T. Swain, Ed. (Academic Press, London, 1963), p. 187.
20. Mass spectra were determined on a modified CEC 21-103C mass spectrometer (for details of modifications and performance, see F. C. Walls and A. L. Burlingame, *Anal. Chem.*, submitted) equipped with heated glass inlet system operated at 200°C. All spectra were determined at ionizing voltage of 70 ev, ionizing current at 10 μa and 160 to 180 volts per stage on the multiplier.
21. This work supported by NASA (grant 101-61) and by the AEC. We thank Dr. P. E. Cloud, Jr., of the University of Minnesota and the owners and geologists of the White Pine Copper Mine, White Pine, Ontonagon County, Michigan, for providing the samples and for the information pertaining to them. We thank Dr. W. E. Robinson, Bureau of Mines, Laramie, Wyoming, for providing the Colorado oil shale.

* NATO fellow, 1962–64.

15 May 1964

Shape of the Recorded Area in Precession Photographs and Its Application in Orienting Crystals

Abstract. *The equation of the perimeter of the recorded area of zero-level precession photographs as a function of the orientation error is derived in polar coordinates. The angle between the tangent to the perimeter and the radius vector is also derived. How these relations can be conveniently applied to determining the orientation error of a crystal mounted on the precession instrument is discussed.*

The recorded region of a zero-level precession photograph is marked out by general-radiation streaks (1). When the crystal is properly oriented this shaded region is circular with its center at the location of the 000 reflection. If the crystal is somewhat misoriented the edges of the recorded region shift in the direction of the setting error. This is the basis for various methods of correcting an orientation error (1, 2, 3).

The knowledge of the shape of the recorded area for precession photographs made with a somewhat misoriented crystal is in a confused state. Fisher (2) considers the area to coincide with a "circle of precession" on the side of error, but shortened on the opposite side (2, p. 1039). Furthermore, although the feature is not discussed, a central region without a record is evident in his Fig. 34a. Evans (3) illustrates such a region in a drawing, but also without discussion and, as will be seen subsequently, the shapes of the bounding curves are misleading.

In the first publication on the precession method (1) the change in radius due to an orientation error was derived. When the law of sines is applied to the triangle *OWJ* of Fig. 13 (1, p. 24) of that article it is seen that

$$\frac{\xi_{\max}}{2 \sin(\bar{\mu} + \epsilon)} = \frac{\sin(90^\circ + \bar{\mu} + \epsilon)}{\sin(90^\circ - \bar{\mu} - 2\epsilon)} \quad (1)$$

which can be solved for ξ_{\max} to give

$$\xi_{\max} = \frac{\sin 2(\bar{\mu} + \epsilon)}{\cos(\bar{\mu} + 2\epsilon)} \quad (2)$$

The maximum radius vector ξ_{\max} occurs when the phase of the precession motion brings the angle $\bar{\mu}$ in the same direction as the error angle ϵ . For present purposes let the phase τ of the precession cycle be measured from the position where the plane of $\bar{\mu}$ is parallel to the plane of ϵ , the angles increasing in the same sense. In the general case the angular separation in the plane of

$\bar{\mu}$ between the misoriented plane and the correctly oriented one is ε' . The plane of $\bar{\mu}$ is always normal to the correct position of the reciprocal-lattice plane. Since the arcs ε' and τ are orthogonal, the relation of ε' to τ and ε is

$$\varepsilon' = \tan^{-1}(\cos \tau \tan \varepsilon) \quad (3)$$

If ε in Eq. 2 is replaced by ε' , and then Eqs. 2 and 3 are combined the result is

$$\xi = \frac{\sin 2(\bar{\mu} + \tan^{-1}[\tan \varepsilon \cos \tau])}{\cos(\bar{\mu} + 2 \tan^{-1}[\tan \varepsilon \cos \tau])} \quad (4)$$

Some representative shapes of the recorded region as provided by Eq. 4 are illustrated in Fig. 1 for $\bar{\mu} = 10^\circ$. Since τ occurs in Eq. 4 as $\cos \tau$, all curves are symmetrical about $\tau = 0$ and $\tau = 180^\circ$. When $\tau = 90^\circ$, Eq. 3 reduces to $\varepsilon' = 0$; at this azimuth the misoriented and oriented plane coincide (that is, intersect). Thus, regardless of the orientation error ε , the two radius vectors at right angles to the direction of the error have a constant length equal to $\xi = 2 \sin \bar{\mu}$. This was discovered empirically by Fisher (2) who noted that a series of reciprocal-lattice planes in a zone are recorded in such a way as to have a common chord.

Interesting and characteristic features occur in the side opposite the orientation error, that is, in the region from $\tau = 90^\circ$ to $\tau = 270^\circ$. When the orientation error is small, this side of the shaded region is merely flattened; at errors approaching $\varepsilon = \bar{\mu}$ it becomes indented, and at $\varepsilon = \bar{\mu}$ a cusp occurs so that ξ becomes zero at $\tau = 180^\circ$. When $\varepsilon > \bar{\mu}$, the numerator of Eq. 4 becomes negative in the neighborhood of $\tau = 180^\circ$ while the denominator remains positive, so that ξ becomes negative. Under these circumstances, an area without a record, here called a blind region, develops within the outer perimeter of the recorded region.

These features can be treated analytically by a second method. A convenient measure of the shape is provided by the angle ψ which the tangent to the boundary makes with the radius vector ξ at the point of tangency. The general relation between ψ , ξ , and τ is

$$\tan \psi = \xi / \left(\frac{\partial \xi}{\partial \tau} \right). \quad (5)$$

The term in the denominator is given by differentiating Eq. 4:

$$\frac{\partial \xi}{\partial \tau} = - \frac{2 \tan \varepsilon \sin \tau \cos \bar{\mu}}{\cos^2(\bar{\mu} + 2 \tan^{-1}[\tan \varepsilon \cos \tau]) (1 + \tan^2 \varepsilon \cos^2 \tau)}. \quad (6)$$

Thus the specific form of Eq. 5 for the boundary of the shaded region is

$$\tan \psi = - \frac{\xi \cos^2(\bar{\mu} + 2 \tan^{-1}[\tan \varepsilon \cos \tau]) (1 + \tan^2 \varepsilon \cos^2 \tau)}{2 \tan \varepsilon \sin \tau \cos \bar{\mu}}. \quad (7)$$

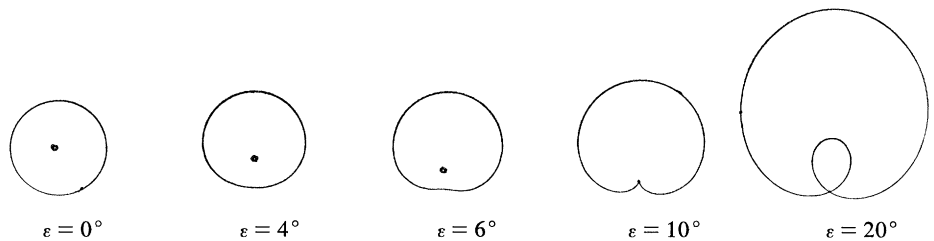


Fig. 1. The shapes of the recorded region for various orientation errors ε , for $\bar{\mu} = 10^\circ$. The direction of the error ($\tau = 0$) is up.

If the angle on the origin side of the tangent is required the sign of Eq. 7 is changed.

This general expression is cumbersome. An important special case occurs for the direction $\tau = 90^\circ$, when Eq. 7 reduces to

$$\tan \psi_{(\tau=90^\circ)} = \frac{\sin 2\bar{\mu}}{2 \tan \varepsilon} \quad (8)$$

The magnitudes of ξ which occur at $\tau = 0^\circ$ and $\tau = 180^\circ$ may be called ξ_{\max} and ξ_{\min} respectively (Fisher's δ is an approximation to ξ_{\max}). These extreme values when plotted against the error are useful in determining orientation errors. With such a plot either ξ_{\max} and ξ_{\min} , or both, may be used to establish the orientation error. In practice, however, when $\varepsilon \approx \bar{\mu}$, the perimeter of the shaded region near $\tau = 180^\circ$ falls within the shadow of the direct-beam stop so that ξ_{\min} cannot be determined.

When the orientation error is so large that the edge of the shaded area falls beyond the edge of the film, ξ_{\max} can no longer be determined. But for a considerable range beyond this, the edge of the blind spot is still within the film, so that the orientation error can be determined with the aid of ξ_{\min} . It may be noted that whereas the use of a smaller value of $\bar{\mu}$ allows the correction of a larger error when measuring ξ_{\max} , the opposite holds when measuring ξ_{\min} , the larger the value of $\bar{\mu}$, the larger the allowable error.

The curvature of the boundary of the shaded region at $\tau = 90^\circ$ can be readily measured and provides an alternative means of determining the orientation error. This is especially important for large errors when the edge of the blind area is outside the film; under these circumstances the boundary curvature

at $\tau = 90^\circ$ can still be measured, so the error can be determined. In fact the use of Eq. 8 permits determining an orientation error of any size provided only that the zero-level reciprocal-lattice plane is sufficiently prominent so that it has an appreciable shading. Furthermore, in methods involving the relation of ξ to ε as in Eq. 4, or of $\Delta\xi$ to ε , as in the case of Evans' method (3), the relation cannot be solved for ε analytically, so that one is forced to use graphical methods. On the other hand Eq. 8 can be readily solved for ε .

A practical procedure for determining the orientation error by this means is as follows: A circle centered at the origin and of radius $2M \sin \bar{\mu}$, where M is the crystal-to-film distance, is scratched on the film with a pair of dividers.

The intersections of this scratched circle with the outside of the recorded region occur at the end of the common chord. The angle between the common chord and the tangent to the recorded region at either intersection point is the angle ψ which should be measured. The relation of Eq. 8 may then be used to determine the magnitude of ε ; the direction of the error is normal to the common chord and toward the larger side of the shaded region. To correct this error it must ordinarily be partitioned between the dial and the goniometer arcs.

M. J. BUERGER

WAYNE A. DOLLASE

*Crystallography Laboratory,
Massachusetts Institute of Technology,
Cambridge*

References and Notes

1. M. J. Buerger, *Photography of the Reciprocal Lattice* (American Crystallographic Association, Monograph No. 1, 1944).
2. D. J. Fisher, *Am. Mineralogist* **37**, 1036 (1952).
3. H. T. Evans, in *International Tables for X-Ray Crystallography*, J. S. Kasper and K. Lonsdale, Eds. (Kynoch Press, Birmingham, 1959), pp. 194-200.
4. We thank Dr. H. Onken for writing the program for computing values of Eq. 4 which were used in Fig. 1. The computations were carried out by Onken on the IBM 7094 computer at the M.I.T. Computation Center. This investigation was supported by a grant from the NSF.

25 March 1964